

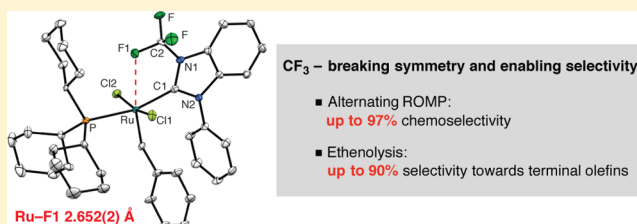
N-Trifluoromethyl NHC Ligands Provide Selective Ruthenium Metathesis Catalysts

Pascal S. Engl, Alexey Fedorov, Christophe Copéret, and Antonio Togni*

Department of Chemistry and Applied Biosciences, ETH Zürich, Vladimir-Prelog-Weg 2, CH-8093 Zürich, Switzerland

Supporting Information

ABSTRACT: We report the synthesis of ruthenium metathesis catalysts containing unsymmetrical *N*-trifluoromethyl NHC ligands. These complexes have been fully characterized, and a Ru–F interaction has been identified in the solid state by X-ray crystallographic analysis for three catalysts with Ru–F distances between 2.629(2) and 2.652(2) Å. The influence of the *N*-trifluoromethyl NHC ligands on the initiation rates and activation parameters was studied. The activity of these catalysts was evaluated in benchmark olefin metathesis reactions and compared to the standard second-generation Grubbs catalyst. Remarkably, *N*-trifluoromethyl catalysts display an unusually high selectivity for the formation of terminal olefins (up to 90%) in the ethenolysis of ethyl oleate. Much improved selectivity is demonstrated for alternating copolymerization of cyclooctene and norbornene as well. These results underline the importance of electronic effects exerted by the NHC ligand.



INTRODUCTION

Over the last decades, transition-metal-catalyzed olefin metathesis has emerged as a powerful synthetic tool for the construction of carbon–carbon double bonds.^{1,2} Research has focused on finding highly active and stable well-defined catalysts. In the specific case of Ru, the first breakthroughs were the identification of $\text{Cl}_2\text{Ru}(\text{=CHR})(\text{PR}_3)_2$ as active metathesis catalysts.³ The second one was the introduction of *N*-heterocyclic carbene (NHC) supporting ligands,⁴ such as 1,3-bis(2,4,6-trimethylphenyl)-4,5-dihydroimidazol-2-ylidene (H_2IMes) in the so-called second-generation Grubbs catalyst (**1**, Figure 1).⁵ Such catalysts combine high olefin metathesis

relevant intermediates.⁹ Metathesis catalysts such as **1** contain the phosphine ligand *trans* to the NHC at a latent substrate binding site. While H_2IMes is a poor π acceptor, its replacement by NHC ligands with greater π acceptor capacity has been proposed to attenuate competing Ru– PCy_3 π -back-donation, thereby stabilizing the Ru– PCy_3 bond and facilitating catalyst initiation.¹⁰ Currently, the development of selective catalysts is one of the most challenging aspects of olefin metathesis. Most recent research efforts led to the discovery of *Z*-selective catalysts.^{6b,11} Another, perhaps less recognized yet important aspect is the development of chemoselective catalysts. One of the early examples was the discovery of selective alternating copolymerization catalysts based on bidentate P,O ligands.^{12,13} Ruthenium catalysts supported by unsymmetrical NHC ligands also show improved selectivities in the ring-opening–ring-closing metathesis reactions compared to **1**.¹⁴ In recent developments cyclic alkyl amino carbene (CAAC) ligands gave Ru metathesis catalysts such as **2** (Figure 1) with exceptional activity and improved selectivity in ethenolysis reactions.^{8a,15}

NHC ligands can be readily fine-tuned via substitution in the backbone or at the nitrogen atoms to tailor catalyst properties.¹⁶ For instance, asymmetry can be installed in the metathesis catalyst through a Ru–F interaction, which was proposed to occur in complex **3** after PCy_3 dissociation.¹⁷ The superior catalytic efficiency of **3** in ring-closing metathesis as compared to **1** was explained via such Ru–F interaction, which reduced the activation energy of the rate-limiting PCy_3 dissociation required to initiate the catalytic cycle.¹⁷ Unex-

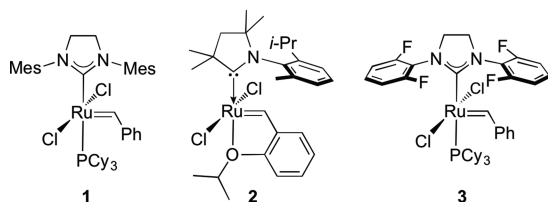
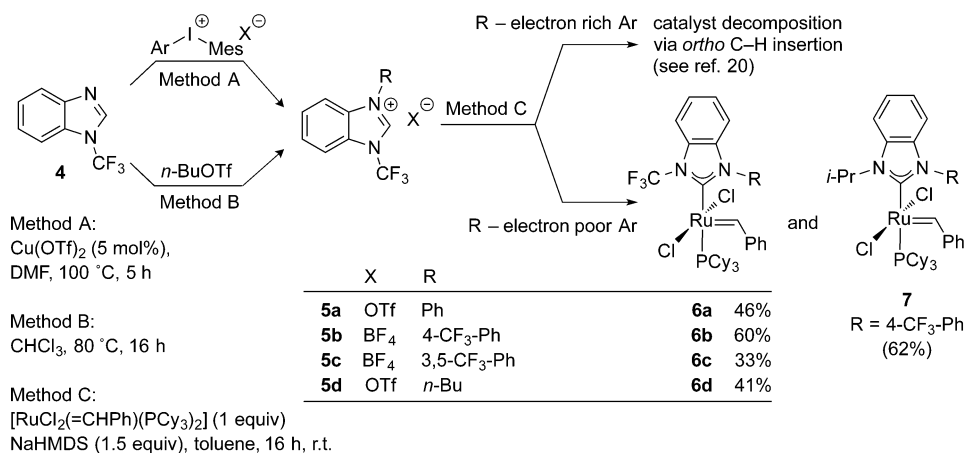


Figure 1. Ruthenium olefin metathesis catalysts **1**–**3**. Cy, cyclohexyl; Mes, mesityl.

activity with functional group tolerance as well as good air and moisture stability. This enabled numerous applications including the synthesis of natural products and bioactive compounds,⁶ advanced materials,⁷ and industrial-scale production of olefins from biomass-derived olefinic feedstocks.⁸ The high stability and remarkable performance of **1** are attributed to the enhanced σ -donor ability of the supporting NHC ligand, which provides strong metal–carbon bonds and stabilizes both the precatalyst and coordinatively unsaturated, catalytically

Received: January 13, 2016

Scheme 1. Synthesis of Ru Benzylidenes **6a–d** and Structure of **7**

explored in catalysis are unsymmetrical NHC ligands with one *N*-trifluoromethyl substituent,¹⁸ which could provide beneficial effects because the strongly electron withdrawing CF₃ group imposes electronic and steric bias on the NHC ligand. The fluorine–metal interaction^{17,19} in such complexes is predetermined by the ligand design. Here we describe the synthesis and the catalytic activity of a series of Ru olefin metathesis catalysts containing *N*-trifluoromethyl benzimidazolide NHC ligands with the goal to develop chemoselective catalysts. We focused on alternating copolymerization of cyclic olefins and selective synthesis of terminal olefins in ethenolysis of ethyl oleate. From the catalysis standpoint, the important result is significantly improved chemoselectivity displayed by our catalysts in these reactions.

RESULTS AND DISCUSSION

Synthesis of Ru NHC Benzylidene Complexes.

Benzimidazolium salts **5a–d** (Scheme 1) were synthesized via electrophilic arylation or alkylation of *N*-trifluoromethyl benzimidazole **4**. Complexes **6a–d** were then obtained in moderate to fair yields by *in situ* deprotonation of the salts **5a–d** with NaHMDS in toluene in the presence of stoichiometric [RuCl₂(=CHPh)(PCy₃)₂] (Scheme 1). Benzylidene **7** was synthesized analogously and used as a *N*-CF₃-free benchmark catalyst with a benzimidazolide NHC framework (see the SI for details). The majority of Ru metathesis catalysts with NHC ligands contain *ortho*-substituents on the *N*-aryl groups, necessary to avoid catalyst decomposition through *ortho* C–H activation.^{19a,20,21} We initially tested several diaryliodonium salts with *ortho*-substituted aryl groups in arylation of **4** but observed no formation of the respective NHC salts. As diaryliodonium salts that are devoid of *ortho* aryl substitution proved competent arylation reagents, we resorted to using electronic rather than steric effects to suppress the aforementioned *ortho* C–H insertion pathways deactivating Ru complexes. Toward this end we installed electron-neutral or electron-depleted aryl groups on the benzimidazolium ligand, providing stable Ru benzylidenes **6a–c** and **7**. In addition, the alkyl analogue **6d** was prepared to evaluate the influence of aryl vs alkyl substitution. Complexes **6a–d** and **7** are air stable in the solid state but slowly decompose in solution at room temperature. All complexes were characterized by NMR spectroscopy, IR, elemental analysis, and HRMS.

Single crystals of **6a,b,d** suitable for X-ray analysis were obtained from the respective CH₂Cl₂ solution by slow diffusion

of hexane. In the solid state both **6a** and **6d** (see the SI for the related structure of **6b**) exhibit a square pyramidal geometry that is distorted toward octahedral structure with the benzimidazolium ring bisecting the Cl–Ru–Cl angle and the *N*-aryl (**6a,b**) and the *N*-*n*-butyl (**6d**) groups almost in a plane that is parallel to the benzylidene ligand (Figures 2 and S24–26). The C2–F1 bonds of the *N*-trifluoromethyl groups are nearly in plane with the heterocycle (the torsion angle C1–N1–C2–F1 is 18.9(5)° for **6a** and 11.0(3)° for **6d**), which

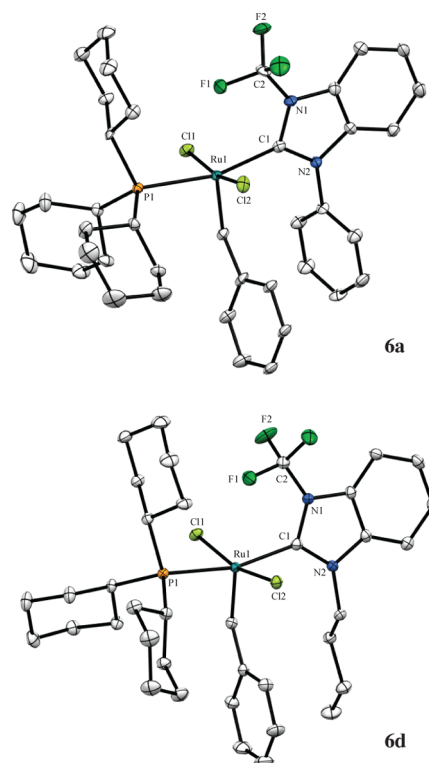


Figure 2. Ortep drawings of **6a** and **6d**. Hydrogen atoms are omitted for clarity, and thermal ellipsoids are set to 50% probability. Selected bond lengths [Å], bond angles [deg], and torsion angles [deg] for **6a**: Ru1–F1 2.652(2), C2–F1 1.335(4), C2–F2 1.324(5), N1–C1–Ru1 123.1(2), N2–C1–Ru1 133.5(3), Cl1–Ru1–Cl2 168.28(2), C1–N1–C2–F1–18.9(5). For **6d**: Ru1–F1 2.629(2), C2–F1 1.332(3), C2–F2 1.328(3), N1–C1–Ru1 121.44(15), N2–C1–Ru1 134.32(16), Cl1–Ru1–Cl2 166.56(2), C1–N1–C2–F1 11.0(3).

places the fluorine atom close to the ruthenium center. The Ru–F distances in **6a** (2.652(2) Å) and **6d** (2.629(2) Å) are significantly shorter than the sum of the van der Waals radii of ruthenium and fluorine (3.52 Å). In addition, the C2–F1 bond (1.335(4) Å for **6a** and 1.332(3) Å for **6d**) is elongated when compared to the C2–F2 bond (1.324(5) Å for **6a** and 1.324(5) Å for **6d**), while the NHC ligand is slightly tilted toward the side occupied by the *N*-trifluoromethyl group (N1–C1–Ru1 123.1(2)° vs N2–C1–Ru1 133.5(3)° for **6a** and N1–C1–Ru1 123.1(2)° vs N2–C1–Ru1 133.5(3)° for **6d**). The latter could be aided by electrostatic interactions in the case of the *N*-phenyl complex **6a**. However, the closely related molecular structure of the *N*-*n*-butyl complex **6d** suggests that it is the Ru–F interaction that determines such geometry.

¹H NMR spectroscopy indicated that for all complexes **6a–d** only a single rotational isomer is present in solution. 2D ¹H/¹H NOESY NMR spectra contain a cross-peak between the benzylidene proton and the *N*-aryl *ortho*-hydrogens in **6a–c** and the *N*-*n*-butyl methylene hydrogens in **6d** (Figures S20–23, SI), suggesting that the solid-state geometry is also preferred in solution.

Initiation Studies. Detailed studies by Grubbs have revealed a complex relationship between phosphine dissociation rates and the catalyst activity.^{14d,22} In order to further evaluate the influence of the *N*-trifluoromethyl group on the properties of **6a–d** and **7**, we determined the activation parameters of phosphine dissociation via quantitative and irreversible reaction of these complexes with butyl vinyl ether (BVE) in benzene-*d*₆ and compared the obtained values with those of **1** and **3**. The disappearance of the starting benzylidene signal of **6a–d** and **7** in the presence of 30 equiv of BVE was monitored by ¹H NMR at different temperatures as a function of time and showed clean first-order kinetics over a period of at least three half-lives. The initiation rate constants were found to be independent of the concentration of BVE, thereby indicating that phosphine dissociation is rate limiting in the initiation step. The activation parameters were extracted via analysis of respective Eyring plots and are summarized in Table 1. The decrease of the free energy of activation ΔG^\ddagger for the initiation step of **3** with respect to **1** has previously been associated with a Ru–F interaction (Table 1, entries 1, 2).¹⁷

In contrast, catalysts **6a–d** and **7** displayed free energies of activation indistinguishable from that of **1** within experimental error. This indicates that the labilization of the Ru–PCy₃ bond due to the Ru–F interaction and greater π acceptor capacity of the unsaturated benzimidazolium NHC framework is offset by another effect, such as the substantially weaker σ electron

donation and hence weaker *trans* influence of the benzimidazolide NHC ligand compared to the imidazolium one.¹⁸

The most striking difference can be noted between the entropy of activation ΔS^\ddagger of N–CF₃ catalyst **6b** and its *N*-*i*Pr analogue **7** (Table 1, entries 4 and 7). This may reflect the influence of the alkyl vs aryl *N*-group, as catalyst **6d**, containing N–CF₃, features low ΔS^\ddagger as well (Table 1, entry 6). While catalysts **6a–c** demonstrate activation entropies ΔS^\ddagger typical for the generally accepted dissociative mechanism, the significantly lower ΔS^\ddagger values of catalysts **6d** and **7** might hint toward a change of the catalyst activation pathway. However, as was mentioned earlier, the initiation rate constants of **6d** and **7** are independent of olefin concentration, which excludes an associative or interchange mechanism.²³ The lower values for ΔS^\ddagger can therefore be tentatively ascribed to a reduced degree of solvent reorganization around the *N*-alkyl rather than *N*-aryl groups in the transition state leading to phosphine dissociation. In addition, the enthalpies of activation ΔH^\ddagger are also lower for catalysts **6d** and **7** (Table 1, entries 6, 7). This is likely due to the increased electron-donating ability of NHC ligands bearing *N*-alkyl groups (**6d** and **7**) and therefore a stronger *trans* effect, which weakens the ruthenium phosphine bond.²⁴

Benchmarking of Activity in Ring-Closing Metathesis (RCM) and Cross-Metathesis (CM) Reactions. We initially tested **6a–d** and **7** in the model ring-closing reaction of diethyl diallylmalonate (**8**) and compared their catalytic activity to the benchmark second-generation Grubbs catalyst **1**.²⁵ The reactions were carried out in CD₂Cl₂ with 1 mol % catalyst loading, and conversion to cycloalkene **9** was monitored by ¹H NMR spectroscopy. Although **6a–d** were competent catalysts in the RCM of **8**, longer reaction times were required when compared to **1** (Figure 3). Catalysts **6a–c** exhibit an identical

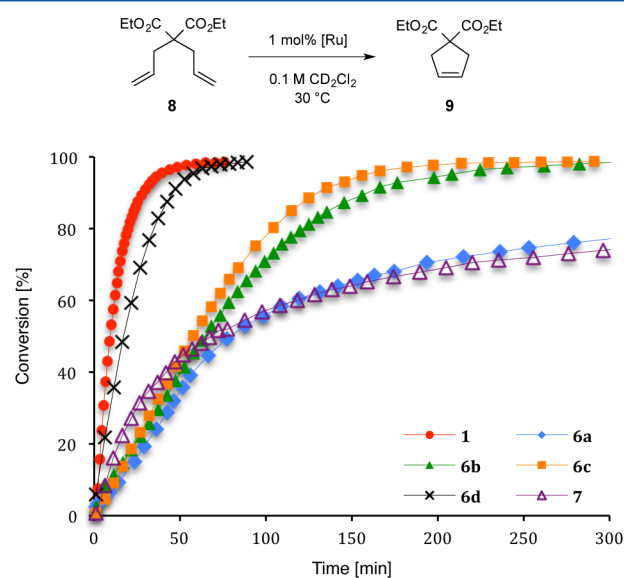


Figure 3. RCM reaction of **8** with catalysts **1**, **6a–d**, and **7** monitored by ¹H NMR spectroscopy.

kinetic profile in the first 50 min; however, while **6b** and **6c** reach >97% conversion, the activity of **6a** drops with time. Catalysts bearing small alkyl *N*-substituents on the NHC ligand are known to be highly reactive; however their stability in solution is also decreased.²⁶ Interestingly, while the *N*-trifluoromethyl and *N*-isopropyl groups are sterically similar,²⁷ the replacement of CF₃ in **6b** by *i*-Pr in **7** results in significantly

Table 1. Activation Parameters for **1**, **3**, **6a–d**, and **7**^a

entry	[Ru]	ΔH^\ddagger [kcal mol ⁻¹]	ΔS^\ddagger [cal K ⁻¹ mol ⁻¹]	ΔG^\ddagger_{303K} ^b [kcal mol ⁻¹]
1	1	27 ± 2	13 ± 6	23.0 ± 0.4 ²²
2	3	27 ± 2	19 ± 9	21.8 ± 0.1 ^{14d}
3	6a	27 ± 1	16 ± 2	22 ± 1
4	6b	30 ± 1	22 ± 3	23 ± 1
5	6c	28 ± 2	18 ± 4	22 ± 2
6	6d	24 ± 2	4 ± 3	22 ± 2
7	7	24 ± 2	0 ± 4	23 ± 2

^aReaction conditions: [Ru] = 0.0106 mmol, BVE = 0.318 mmol, ferrocene (3 μmol as an internal standard) in 0.6 mL of C₆D₆ at temperatures from 303 to 330 K. ^bExtrapolated from the Eyring equation.

diminished RCM activity (Figure 3). The superior activity of catalyst **6b** is possibly due to greater catalyst stability toward deactivation through C–H bond insertion pathways.^{19a,20,28} Unexpectedly, catalyst **6d**, with an *N*-*n*-butyl group, outperforms analogous catalysts **6a–c**, exhibiting activity on par with the benchmark catalyst **1**.

We next assessed our catalysts in the cross-metathesis reaction of allylbenzene **10** and *cis*-1,4-diacetoxy-2-butene **11**. Catalysts **6a–d** display activities lower than both **1** and **7** (>87% and >80% conversion, respectively, Figure 4). While

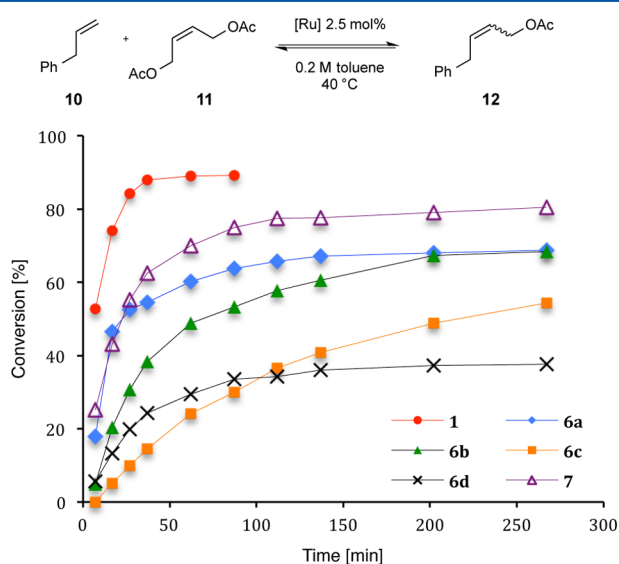


Figure 4. Cross-metathesis of **10** and **11** with catalysts **1**, **6a–d**, and **7**. For selectivity data, see Table S1 and Figure S6 in the SI.

catalyst **6d** showed the highest activity in the RCM reaction, it is a rather poor CM catalyst, reaching only 37% conversion to the cross-product **12**. Catalyst **6a** is more efficient in the CM reaction, leading to 68% conversion to **12**.

Alternating Ring-Opening Metathesis Polymerization (ROMP). In 2005, Chen and co-workers reported the sequence-selective ROMP of *cis*-cyclooctene **13** (COE) and norbornene **14** (NBE) by a mechanistically designed ruthenium carbene complex.^{12,13} Buchmeiser and co-workers used Grubbs-type complexes bearing unsymmetrical NHC ligands for the synthesis of alternating copolymers as well.²⁹ In both cases, the control over alternating copolymerization was aided by optimizing the ratio of comonomers **13** and **14**. Catalyst **1** readily but unselectively polymerizes a mixture of **13** and **14** to give respective homopolymers. We evaluated the catalytic activity and sequence selectivity of catalysts **6a–d** and **7** in the ROMP of a 50:1 mixture of COE and NBE. The polymers obtained were characterized by ¹H and ¹³C NMR spectroscopy (Table 2). The nature of the *N*-substituents of the NHC ligand has a profound influence on the chemoselectivity of these catalysts. Catalysts **6a–c** with *N*-aryl substituents gave copolymers with 85–96% alternating diads after 15 min of the reaction (Table 2, entries 2–4). The alternating copolymer can be obtained with 97% chemoselectivity by reducing the reaction time from 15 min to 5 min, as shown for catalyst **6a** (Table 2, entry 1 and Figure 5). The copolymer obtained with **6d** (Table 2, entry 5) contained a greater amount of the homopolymers, suggesting that the *N*-aromatic ring of the NHC ligand influences chemoselectivity. Remarkably, while **6b**

Table 2. Alternating Copolymerization of COE (**13**) and NBE (**14**)^{a,b}

entry	[Ru]	conversion [mmol] ^c		poly- 13 [%] ^d	poly- 14 [%] ^d	15 [%] ^d
		COE	NBE			
1 ^e	6a	0.131	0.131	3	–	97 (64)
2	6a	0.289	0.262	5	–	95 (62)
3	6b	0.099	0.086	4	–	96 (65)
4	6c	0.068	0.061	7	8	85 (61)
5	6d	0.186	0.149	8	13	79 (64)
6	7	0.199	0.129	53	–	47 (61)

^aReaction conditions: NBE = 0.42 mmol, COE = 21 mmol, [Ru] = 2.1 × 10^{−4} mmol in 7 mL of CH₂Cl₂ at 30 °C for 15 min. ^bLow solubility of polymers did not allow collecting the GPC data. ^cConversions calculated from the consumed moles of norbornene and cyclooctene. ^dDetermined by ¹³C NMR spectroscopy. ^eReaction time was 5 min.

provides a copolymer with 96% alternating diads, its fluorine-free analogue **7** furnishes only 47% alternating copolymerization (Table 2, entry 6). This is possibly due to the increased rotation barrier around the NHC–Ru axis³⁰ in **6b** due to the Ru–F interaction and/or due to the increasing COE:NBE ratio and is in accordance with the observation of the kinetic selectivity at lower conversion and time (Table 2).^{13b,28} The *cis*-selectivity lies within a 60–65% range for all initiators **6–7**, which is typical for the NBE-*alt*-COE polymers prepared with Ru initiators supported by NHC ligands.^{29,31} Interestingly, poly-COE formed in copolymerization experiments along with **15** contains an unusually high amount of *cis* double bonds, amounting to 67% in the case of **7** (Figure 5). Such *cis* content is difficult to achieve with monocyclic olefins even using a new generation of powerful *Z*-selective Ru metathesis catalysts,³² as these monomers are prone to chain transfer reactions and secondary metathesis events.³³ The observed *cis* selectivity is not inherent to **7** and is also found in the polymerization of pure COE using *N*-CF₃ initiator **6b**, which gives 68% *cis* double bonds when used at 500 ppm loading (Table S2). However, when the catalyst loading was increased to 1 mol %, the *cis*-selectivity dropped significantly to 23%, reflecting double-bond isomerization via secondary metathesis events. Lowering the reaction temperature from 30 °C to 0 °C improved the *cis* content to 45%, although at the expense of polymer yield (Table S2).

Ethenolysis of Ethyl Oleate. Cross-metathesis of internal olefins with ethylene, also called ethenolysis, has been receiving increased attention since it allows the synthesis of terminal olefins from sustainable bioderived olefinic feedstock.^{8,34} Such terminal olefins are highly valuable for the chemical industry³⁵ and as a source of renewable biofuels.³⁶ Recently, extremely high turnover numbers up to 340 000 with 1 ppm catalyst loadings were reported for ethenolysis of ethyl oleate using Ru catalysts with advanced cyclic alkyl amino carbene ligands.^{8a} We tested catalysts **6a–d** and **7** in ethenolysis of ethyl oleate **16** and compared their activity to that of catalyst **1**. All catalytic tests were performed by injecting 100 ppm catalyst in toluene to neat **16** pressurized to 10 bar ethylene (isobaric conditions)

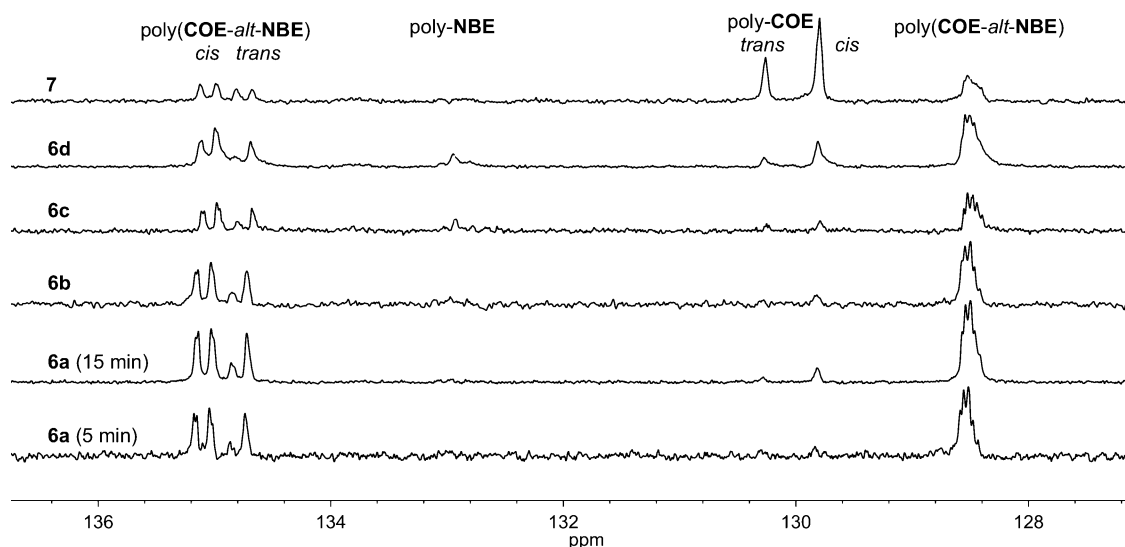


Figure 5. ^{13}C NMR spectra for the polymers presented in Table 2.

at 60 °C, and the reaction progress was monitored via ethylene uptake at constant pressure. Benchmark catalyst **1** achieves nearly full conversion (>97%) of ethyl oleate **16** in less than 10 min according to the gas uptake curve (Figure 6), but also

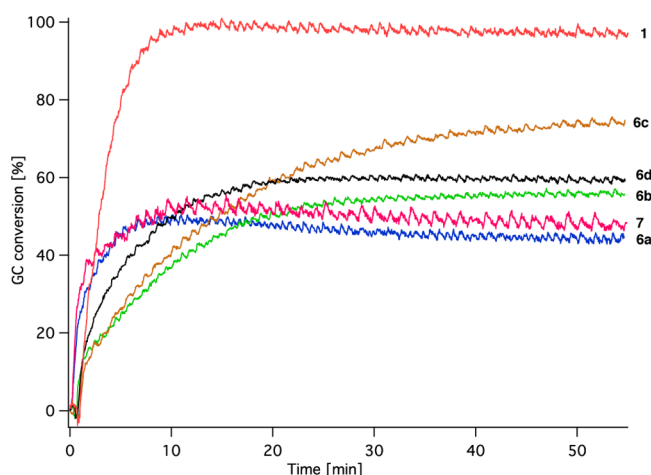
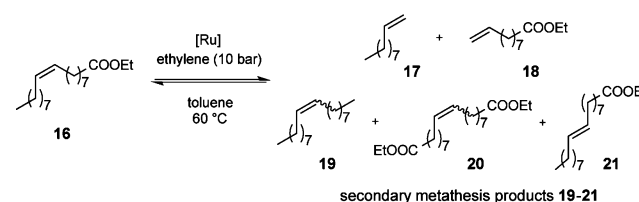


Figure 6. Gas uptake curves for the ethenolysis of ethyl oleate **16** with catalysts **1**, **6a–d**, and **7** at 100 ppm [Ru] loading. The y-axis was back calibrated from GC data of the reaction mixtures.

affords a relatively high amount of secondary metathesis products **19–21**, which substantially lowers the yield of terminal olefins (60%, Table 3, entry 1). Although only moderate to fair conversion of **16** was observed for catalysts **6b–d** (57–74%), they display a remarkably high selectivity (80–90%) for the desired ethenolysis products **17** and **18**.

The moderate conversion and selectivity of catalyst **6a**, on the other hand, leads to a yield of only 19%. With a selectivity of 90%, catalyst **6c** outperforms catalyst **1** under these conditions and achieves an overall yield of 69% for the terminal olefins with a TON of 6860. However, at 20 ppm catalyst loading the selectivity of catalyst **6c** as well as the conversion of **16** is significantly reduced, while catalyst **1** maintains its high activity and achieves a TON of 32 018, presumably due to the higher stability of **1**. Remarkably, the replacement of an *N*-isopropyl group in **7** by the *N*-

Table 3. Ethenolysis of Ethyl Oleate **16** with Catalysts **1**, **6a–d**, and **7**^a



entry	[Ru]	loading [ppm]	C [%] ^b	S [%] ^c	Y [%] ^d	TON ^e
1	1	100	97	46	60	5998
2	1	20	95	43	64	32 018
3	6a	100	44	40	19	1901
4	6b	100	57	80	48	4778
5	6c	100	74	90	69	6860
6	6c	20	56	75	43	21 312
7	6d	100	60	89	55	5516
8	7	100	47	26	17	1694

^aReaction conditions: ethyl oleate **16** = 2.802 mmol, [Ru] = 0.28 μmol , 10 bar of C_2H_4 , 2 mL of toluene. ^bConversion = $100 - [(\text{final moles of ethyl oleate}) \times 100 / (\text{initial moles of ethyl oleate})]$. ^cSelectivity = $(\text{moles of ethenolysis product, terminal olefins}) / [2 \times (\text{moles of total product})] \times 100$. ^dYield of terminal olefins = $[\text{conversion} \times \text{selectivity}] / 100$. ^eTON = $\text{yield of terminal olefins} \times [(\text{moles of ethyl oleate}) / (\text{moles of catalyst})]$.

trifluoromethyl group in **6b** results in a 54% increase in the catalyst's selectivity. This high preference of catalysts **6b–d** for the terminal olefins over the internal ones underlines that electronic effects exerted by the NHC ligands could be used for fine-tuning of activity and selectivity, in addition to traditional approaches utilizing sterically hindered NHC ligands.⁸

CONCLUSIONS

A series of new ruthenium metathesis catalysts bearing sterically and electronically unsymmetrical NHC ligands have been synthesized and fully characterized. X-ray crystallographic analysis of complexes **6a,b,d** indicates a Ru–F interaction in the solid state. The initiation rates and activation parameters are consistent with a dissociative initiation mechanism, in which the displacement of the phosphine ligand is rate limiting. The

free energy of activation ΔG^\ddagger of catalysts **6a–d** does not significantly deviate from that of **1**. Although catalysts **6a–d** do not display improved performances in benchmark reactions compared to original catalysts, they show greatly improved chemoselectivity in alternating copolymerization of cyclooctene and norbornene as well as in ethenolysis of ethyl oleate. In particular, **6a** achieves 97% chemoselectivity in alternating copolymerization, while **6b–d** display a remarkably high selectivity (80–90%) for terminal olefins in ethenolysis of ethyl oleate by avoiding the competing homodimerization of primary terminal olefins. Catalyst **6c** gave 90% selectivity for the kinetic over the thermodynamic ethenolysis products in 69% yield, with a TON of 6860. This enhanced selectivity stems from the electronically unsymmetrical nature of the *N*-trifluoromethyl NHCs, as the selectivity is substantially decreased when *N*-CF₃ is replaced with a sterically equivalent *N*-*i*Pr group. We therefore propose that the electronic bias imposed on the NHC ligand by the strongly electron withdrawing CF₃ group and/or a Ru–F interaction is crucial for achieving high selectivity in the sequence-selective ROMP and ethenolysis reactions. It shows that one should be careful in discarding poor catalysts based on benchmark reactions and that it is essential (at this stage) to evaluate catalysts in a broader range of reactions. These encouraging results suggest that improved chemoselective catalysts can be designed, and we are currently exploring this field.

■ ASSOCIATED CONTENT

Supporting Information

The Supporting Information is available free of charge on the ACS Publications website at DOI: 10.1021/acs.organomet.6b00028.

Experimental procedures and characterization of new compounds; Eyring plots for **6a–d** and **7** (PDF)

Crystallographic data for **6a** (CIF)

Crystallographic data for **6b** (CIF)

Crystallographic data for **6d** (CIF)

■ AUTHOR INFORMATION

Corresponding Author

*E-mail: atogni@ethz.ch.

Notes

The authors declare no competing financial interest.

■ ACKNOWLEDGMENTS

The authors are grateful to the Scientific Equipment Program of ETH Zürich and the Swiss National Science Foundation (R'Equip grant 206021_150709/1) for financial support. A.F. thanks Holcim Stiftung for a Habilitation Fellowship. Lukas Sigrist and Dr. Deven P. Estes (both ETH Zürich) are greatly acknowledged for X-ray crystallographic analyses and assistance with the kinetic analysis, respectively.

■ REFERENCES

- (1) (a) Vougioukalakis, G. C.; Grubbs, R. H. *Chem. Rev.* **2010**, *110*, 1746–1787. (b) Hoveyda, A. H.; Zhugralin, A. R. *Nature* **2007**, *450*, 243–251.
- (2) (a) Grubbs, R. H. *Handbook of Metathesis*; Wiley-VCH: Weinheim, Germany, 2014; Vols. 1–3. (b) Grell, K. *Olefin Metathesis: Theory and Practice*, 1st ed.; Wiley: NJ, USA, 2014.
- (3) (a) Schwab, P.; Grubbs, R. H.; Ziller, J. W. *J. Am. Chem. Soc.* **1996**, *118*, 100–110. (b) Schwab, P.; France, M. B.; Ziller, J. W.; Grubbs, R. H. *Angew. Chem., Int. Ed. Engl.* **1995**, *34*, 2039–2041.
- (4) (a) Hopkinson, M. N.; Richter, C.; Schedler, M.; Glorius, F. *Nature* **2014**, *510*, 485–496. (b) Nelson, D. J.; Nolan, S. P. *Chem. Soc. Rev.* **2013**, *42*, 6723–6753.
- (5) (a) Scholl, M.; Ding, S.; Lee, C. W.; Grubbs, R. H. *Org. Lett.* **1999**, *1*, 953–956. (b) Huang, J.; Stevens, E. D.; Nolan, S. P.; Petersen, J. L. *J. Am. Chem. Soc.* **1999**, *121*, 2674–2678. (c) Scholl, M.; Trnka, T. M.; Morgan, J. P.; Grubbs, R. H. *Tetrahedron Lett.* **1999**, *40*, 2247–2250. (d) Ackermann, L.; Fürstner, A.; Weskamp, T.; Kohl, F. J.; Herrmann, W. A. *Tetrahedron Lett.* **1999**, *40*, 4787–4790.
- (6) (a) Mangold, S. L.; Grubbs, R. H. *Chem. Sci.* **2015**, *6*, 4561–4569. (b) Meek, S. J.; O'Brien, R. V.; Llaveria, J.; Schrock, R. R.; Hoveyda, A. H. *Nature* **2011**, *471*, 461–466. (c) McReynolds, M. D.; Dougherty, J. M.; Hanson, P. R. *Chem. Rev.* **2004**, *104*, 2239–2258.
- (7) (a) Elling, B. R.; Xia, Y. *J. Am. Chem. Soc.* **2015**, *137*, 9922–9926. (b) Weitekamp, R. A.; Atwater, H. A.; Grubbs, R. H. *J. Am. Chem. Soc.* **2013**, *135*, 16817–16820. (c) Sveinbjornsson, B. R.; Weitekamp, R. A.; Miyake, G. M.; Xia, Y.; Atwater, H. A.; Grubbs, R. H. *Proc. Natl. Acad. Sci. U. S. A.* **2012**, *109*, 14332–14336. (d) Xia, Y.; Verduzco, R.; Grubbs, R. H.; Kornfield, J. A. *J. Am. Chem. Soc.* **2008**, *130*, 1735–1740.
- (8) (a) Marx, V. M.; Sullivan, A. H.; Melaimi, M.; Virgil, S. C.; Keitz, B. K.; Weinberger, D. S.; Bertrand, G.; Grubbs, R. H. *Angew. Chem., Int. Ed.* **2015**, *54*, 1919–1923. (b) Thomas, R. M.; Keitz, B. K.; Champagne, T. M.; Grubbs, R. H. *J. Am. Chem. Soc.* **2011**, *133*, 7490–7496. (c) Schrodi, Y.; Ung, T.; Vargas, A.; Mkrtumyan, G.; Lee, C. W.; Champagne, T. M.; Pederson, R. L.; Hong, S. H. *Clean. Soil, Air, Water* **2008**, *36*, 669–673. (d) Higman, C. S.; Lummiss, J. A. M.; Fogg, D. E. *Angew. Chem., Int. Ed.* **2016**, *55*, 3552–3565.
- (9) (a) Jacobsen, H.; Correa, A.; Poater, A.; Costabile, C.; Cavallo, L. *Coord. Chem. Rev.* **2009**, *253*, 687–703. (b) Díez-González, S.; Nolan, S. P. *Coord. Chem. Rev.* **2007**, *251*, 874–883. (c) Occhipinti, G.; Bjorsvik, H. R.; Jensen, V. R. *J. Am. Chem. Soc.* **2006**, *128*, 6952–6964.
- (10) Lummiss, J. A. M.; Higman, C. S.; Fyson, D. L.; McDonald, R.; Fogg, D. E. *Chem. Sci.* **2015**, *6*, 6739–6746.
- (11) (a) Herbert, M. B.; Grubbs, R. H. *Angew. Chem., Int. Ed.* **2015**, *54*, 5018–5024. (b) Occhipinti, G.; Hansen, F. R.; Tornroos, K. W.; Jensen, V. R. *J. Am. Chem. Soc.* **2013**, *135*, 3331–3334. (c) Fürstner, A. *Science* **2013**, *341*, 1357–1363. (d) Keitz, B. K.; Endo, K.; Patel, P. R.; Myles, H. B.; Grubbs, R. H. *J. Am. Chem. Soc.* **2012**, *134*, 693–699.
- (12) Bornand, M.; Chen, P. *Angew. Chem., Int. Ed.* **2005**, *44*, 7909–7911.
- (13) (a) Jović, M.; Torker, S.; Chen, P. *Organometallics* **2011**, *30*, 3971–3980. (b) Torker, S.; Muller, A.; Chen, P. *Angew. Chem., Int. Ed.* **2010**, *49*, 3762–3766. (c) Bornand, M.; Torker, S.; Chen, P. *Organometallics* **2007**, *26*, 3585–3596.
- (14) (a) Queval, P.; Jahier, C.; Rouen, M.; Artur, I.; Legeay, J. C.; Falivene, L.; Toupet, L.; Crevisy, C.; Cavallo, L.; Basle, O.; Mauduit, M. *Angew. Chem., Int. Ed.* **2013**, *52*, 14103–14107. (b) Kavitate, S.; Samantaray, M. K.; Dehn, R.; Deuerlein, S.; Limbach, M.; Schachner, J. A.; Jeanneau, E.; Copéret, C.; Thieuleux, C. *Dalton Trans.* **2011**, *40*, 12443–12446. (c) Karamé, I.; Boualleg, M.; Camus, J. M.; Maishal, T. K.; Alauzun, J.; Basset, J. M.; Copéret, C.; Corriu, R. J.; Jeanneau, E.; Mehdi, A.; Reye, C.; Veyre, L.; Thieuleux, C. *Chem. - Eur. J.* **2009**, *15*, 11820–11823. (d) Vougioukalakis, G. C.; Grubbs, R. H. *Chem. - Eur. J.* **2008**, *14*, 7545–7556. (e) Van Veldhuizen, J. J.; Garber, S. B.; Kingsbury, J. S.; Hoveyda, A. H. *J. Am. Chem. Soc.* **2002**, *124*, 4954–4955.
- (15) Anderson, D. R.; Lavallo, V.; O'Leary, D. J.; Bertrand, G.; Grubbs, R. H. *Angew. Chem., Int. Ed.* **2007**, *46*, 7262–7265.
- (16) (a) Samantaray, M. K.; Alauzun, J.; Gajan, D.; Kavitate, S.; Mehdi, A.; Veyre, L.; Lelli, M.; Lesage, A.; Emsley, L.; Copéret, C.; Thieuleux, C. *J. Am. Chem. Soc.* **2013**, *135*, 3193–3199. (b) Khan, R. K.; O'Brien, R. V.; Torker, S.; Li, B.; Hoveyda, A. H. *J. Am. Chem. Soc.* **2012**, *134*, 12774–12779. (c) Xia, Y.; Boydston, A. J.; Grubbs, R. H. *Angew. Chem., Int. Ed.* **2011**, *50*, 5882–5885.

- (17) Ritter, T.; Day, M. W.; Grubbs, R. H. *J. Am. Chem. Soc.* **2006**, *128*, 11768–11769.
- (18) Engl, P. S.; Senn, R.; Otth, E.; Togni, A. *Organometallics* **2015**, *34*, 1384–1395.
- (19) (a) Mathew, J.; Koga, N.; Suresh, C. H. *Organometallics* **2008**, *27*, 4666–4670. (b) Stanek, K.; Czarniecki, B.; Aardoom, R.; Rügger, H.; Togni, A. *Organometallics* **2010**, *29*, 2540–2546. (c) Plenio, H. *Chem. Rev.* **1997**, *97*, 3363–3384.
- (20) (a) Poater, A.; Bahri-Laleh, N.; Cavallo, L. *Chem. Commun.* **2011**, *47*, 6674–6676. (b) Hong, S. H.; Chlenov, A.; Day, M. W.; Grubbs, R. H. *Angew. Chem., Int. Ed.* **2007**, *46*, 5148–5151. (c) Vehlouw, K.; Gessler, S.; Blechert, S. *Angew. Chem., Int. Ed.* **2007**, *46*, 8082–8085.
- (21) Borguet, Y.; Zaragoza, G.; Démonceau, A.; Delaude, L. *Dalton Trans.* **2015**, *44*, 9744–9755.
- (22) Sanford, M. S.; Love, J. A.; Grubbs, R. H. *J. Am. Chem. Soc.* **2001**, *123*, 6543–6554.
- (23) (a) Vorfalt, T.; Wannowius, K. J.; Plenio, H. *Angew. Chem., Int. Ed.* **2010**, *49*, 5533–5536. (b) Engle, K. M.; Lu, G.; Luo, S. X.; Henling, L. M.; Takase, M. K.; Liu, P.; Houk, K. N.; Grubbs, R. H. *J. Am. Chem. Soc.* **2015**, *137*, 5782–5792.
- (24) Pinter, B.; Van Speybroeck, V.; Waroquier, M.; Geerlings, P.; De Proft, F. *Phys. Chem. Chem. Phys.* **2013**, *15*, 17354–17365.
- (25) Ritter, T.; Hejl, A.; Wenzel, A. G.; Funk, T. W.; Grubbs, R. H. *Organometallics* **2006**, *25*, 5740–5745.
- (26) (a) Vehlouw, K.; Maechling, S.; Blechert, S. *Organometallics* **2006**, *25*, 25–28. (b) Grisi, F.; Costabile, C.; Gallo, E.; Mariconda, A.; Tedesco, C.; Longo, P. *Organometallics* **2008**, *27*, 4649–4656.
- (27) (a) Leroux, F. *ChemBioChem* **2004**, *5*, 644–649. (b) Bott, G.; Field, L. D.; Sternhell, S. *J. Am. Chem. Soc.* **1980**, *102*, 5618–5626.
- (28) Herbert, M. B.; Lan, Y.; Keitz, B. K.; Liu, P.; Endo, K.; Day, M. W.; Houk, K. N.; Grubbs, R. H. *J. Am. Chem. Soc.* **2012**, *134*, 7861–7866.
- (29) (a) Lichtenheldt, M.; Wang, D.; Vehlouw, K.; Reinhardt, I.; Kuhnel, C.; Decker, U.; Blechert, S.; Buchmeiser, M. R. *Chem. - Eur. J.* **2009**, *15* (37), 9451–7. (b) Vehlouw, K.; Wang, D.; Buchmeiser, M. R.; Blechert, S. *Angew. Chem., Int. Ed.* **2008**, *47*, 2615–2618.
- (30) Adlhart, C.; Chen, P. *Angew. Chem., Int. Ed.* **2002**, *41*, 4484–4487.
- (31) Buchmeiser, M. R.; Ahmad, I.; Gurram, V.; Kumar, P. S. *Macromolecules* **2011**, *44*, 4098–4106.
- (32) Keitz, B. K.; Fedorov, A.; Grubbs, R. H. *J. Am. Chem. Soc.* **2012**, *134*, 2040–2043.
- (33) Bielawski, C. W.; Grubbs, R. H. *Angew. Chem., Int. Ed.* **2000**, *39*, 2903–2906.
- (34) (a) Patel, J.; Mujcinovic, S.; Jackson, W. R.; Robinson, A. J.; Serelis, A. K.; Such, C. *Green Chem.* **2006**, *8*, 450–454. (b) Patel, J.; Elaridi, J.; Jackson, W. R.; Robinson, A. J.; Serelis, A. K.; Such, C. *Chem. Commun.* **2005**, 5546–5547.
- (35) (a) Lysenko, Z.; Maughon, B. R.; Bicerano, J.; Burdett, K. A.; Christenson, C. P.; Cummis, C. H.; Dettloff, M. L.; Maher, J. M.; Schrock, A. K.; Thomas, P. J.; Varjian, R. D.; White, J. E. WO 2003/093215 A1, priority date of November 13, 2003. (b) Burdett, K. A.; Harris, L. D.; Margl, P.; Maughon, B. R.; Mokhtar-Zadeh, T.; Saucier, P. C.; Wasserman, E. P. *Organometallics* **2004**, *23*, 2027–2047. (c) Mandeli, D.; Jannini, M. J. D. M.; Buffon, R.; Schuchardt, U. *J. Am. Oil Chem. Soc.* **1996**, *73*, 229–232.
- (36) Olson, E. S. US 2010/0191008 A1, priority date of July 29, 2010.